Full Band Calculations of Low-field Mobility in p-type Silicon Nanowire MOSFETs

Neophytos Neophytou, Zlatan Stanojevic, and Hans Kosina
Institute for Microelectronics, TU Wien
Gußhausstraße 27–29 / E360, A–1040 Wien, Austria
E-mail: {neophytou | stanojevic | kosina}@iue.tuwien.ac.at

Abstract— The bandstructure of p-type gated Si nanowires (NWs) is calculated self-consistently using the $sp^3d^5s^*$ atomistic tight-binding (TB) model and the 2D Poisson equation. The Boltzmann transport formalism is then used for calculation of the low-field mobility. We show that the bandstructures of NWs in the [110] and [111] transport orientations change as the channel is driven into inversion, which causes a ~50% increase in their intrinsic phonon-limited hole mobility. For short channel MOSFET devices, however, the total mobility is lower that the intrinsic mobility because it is affected by the so-called "ballistic" mobility.

Keywords—Si nanowires; mobility; transistors; Boltzmann transport; bandstrucutre; "ballistic" mobility

I. INTRODUCTION

Silicon nanowires (NWs) have recently attracted significant attention as candidates for high performance transistor channels [1]. Ultra-scaled NW devices of channel diameters down to D=3nm and lengths as short as 15nm with excellent performance have already been demonstrated by various experimental groups [2, 3, 4, 5]. Furthermore, large mobility and on-current densities in NWs compared to bulk have been observed experimentally [6, 7]. Specifically for ultra-narrow p-type NWs, studies have shown that the carrier velocities and mobilities largely increase as the diameter is reduced down to D=3nm [7, 8, 9]. This was a result of bandstructure changes upon geometrical confinement, and was observed for [111] and [110] NWs. In this work, we show that electrostatic confinement of holes through gating in a MOSFET can also introduce bandstructure variations in these p-type NWs and influence their transport properties.

We calculate the low-field mobility in NWs of diameter D=12nm in the [100], [110] and [111] transport orientations. We use the $sp^3d^5s^*$ tight-binding (TB) model for the electronic structure, self-consistently coupled to the 2D Poisson equation. Upon convergence, the mobility is extracted using linearized Boltzmann transport theory, considering acoustic phonons, optical phonons, and surface roughness scattering. The effective mass of the bands becomes bias dependent, and large increases in the carrier mobility (of the order of ~50%) can be observed in [110] and [111] NWs as the channel is driven into inversion. We finally distinguish the influence of this intrinsic, diffusive mobility from the total "apparent" mobility that would be measured for ultra-scaled channels, and show that the latter will always be lower due to the detrimental effect of the so called "ballistic" mobility.

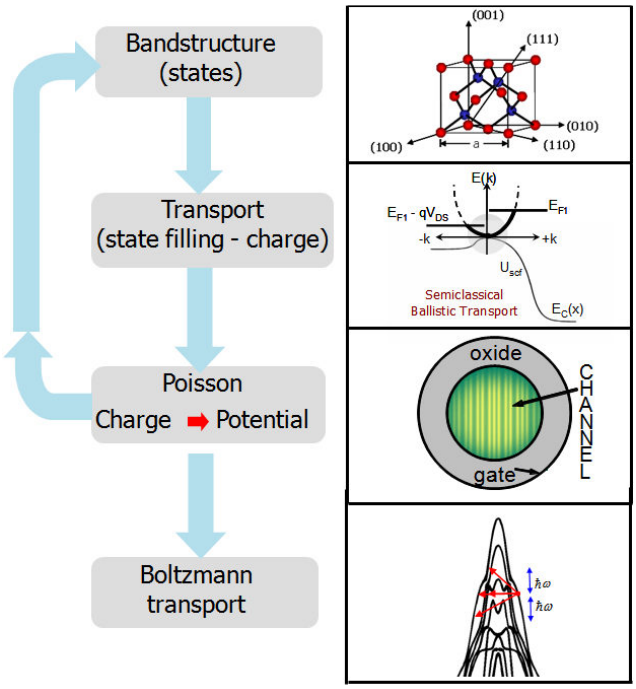

Figure 1: Simulation procedure. (a) The NW bandstructure is calculated using the $sp^3d^5s^*$ TB model. (b) A semiclassical ballistic model is used to calculate the charge distribution in the gated NW. (c) The charge is self-consistently coupled to a 2D Poisson equation for the electrostatic potential in the cross section of the wire. The oxide is assumed to be SiO_2 of thickness t_{ox}=1.2nm (d) Upon convergence (and at V_D=0V), Boltzmann transport theory, including all relevant scattering mechanisms, is used for mobility calculations.

II. APPROACH

To obtain the bandstructure of the NWs we use the nearest neighbor $sp^3d^5s^*$ tight-binding (TB) model, including spin-orbit-coupling [10, 11], which captures all the necessary band features, and in addition, is robust enough to computationally handle larger NW cross sections as compared to ab-initio methods. As an indication, the unit cells of the NWs considered in this study contain up to ~5500 atoms. The computation time needed for the calculation of the self-consistent bandstructure

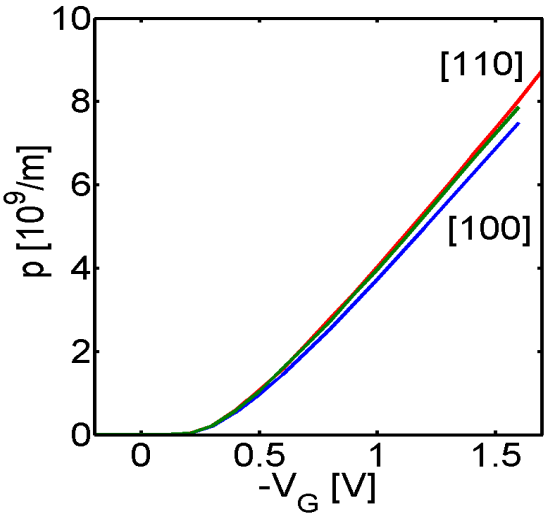

Figure 2: The charge density in the NWs versus gate bias. Quantities for NWs of D=12nm in the [100] (blue), [110] (red) and [111] (green) transport orientations are indicated.

of these NWs can take several days on a single CPU. We consider p-type silicon NWs of D=12nm in three different transport orientations [100], [110], and [111]. The complete computational model is described in Fig. 1. There are four steps in the computation. i) The first step is the calculation of the electronic structure of the NW channel using the TB model. ii) The second step involves the calculation of the charge density using a semiclassical model. The model used is commonly referred to as the "top-of-the-barrier" model [12], and has traditionally been used in calculating the ballistic performance of transistor devices. In this model the positive and negative k-states of the bandstructure are filled according to the Fermi levels of the source and the drain, respectively. In our case, since we calculate low-field mobility using linearized Boltzmann theory, we only have one Fermi level in the entire device which fills both the positive and negative going states equivalently. We chose the Fermi level such that all NWs have the same threshold voltage (in their charge versus voltage characteristics), around V_G=-0.2V. (Note that we use negative gate bias values since we consider p-type channels). This is shown in Fig. 2, which shows the charge density in the cross section of the NWs versus gate bias. Under the same inversion conditions the charge is very similar for the three NWs, because it is controlled by the electrostatics of the channel. Most of the channel capacitance is attributed to the gate capacitance, whereas the influence of the quantum capacitance does not create significant anisotropy in the charge concentration for NWs of different orientations. iii) The third step is the solution of a 2D Poisson equation in the cross section of the NW [13]. A gate all around geometry is used, with 1.2nm SiO_2 as the gate insulator. For this, we include the carrier distribution in the channel, which is determined by summing up the coefficients of the eigenvectors of the various k-states. Finally, upon self-consistent convergence of the bandstructure, we calculate the low-field mobility including acoustic phonons, optical phonons and surface roughness scattering, as described in Ref. [14, 15].

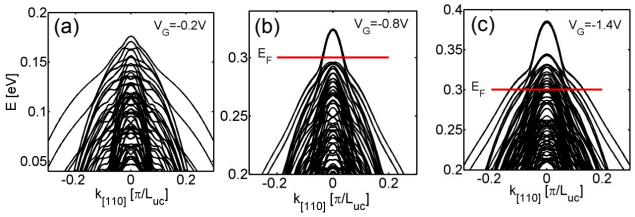

Figure 3: Dispersions of a NW of diameter D=12nm in the [110] transport orientation for different gate biases. (a) V_G=-0.2V (depletion / flat band), ii) V_G=-0.8V (inversion), iii) V_G=-1.4V (strong inversion). The position of the Fermi level in each case is indicated by the red line.

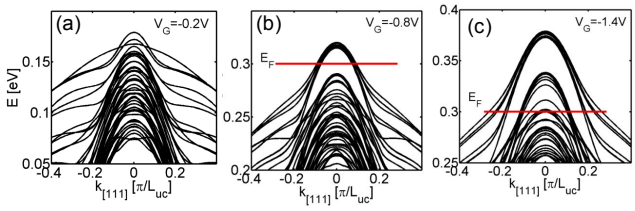

Figure 4: Dispersions of a NW of diameter D=12nm in the [111] transport orientation for different gate biases. (a) V_G=-0.2V (depletion / flat band), ii) V_G=-0.8V (inversion), iii) V_G=-1.4V (strong inversion). The position of the Fermi level in each case is indicated by the red line.

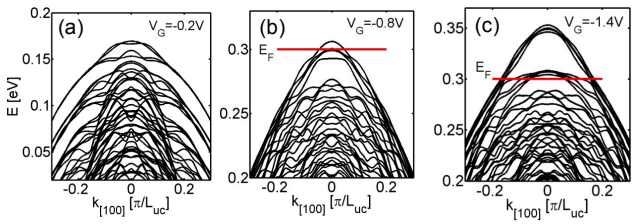

Figure 5: Dispersions of a NW of diameter D=12nm in the [100] transport orientation for different gate biases. (a) V_G=-0.2V (depletion / flat band), ii) V_G=-0.8V (inversion), iii) V_G=-1.4V (strong inversion). The position of the Fermi level in each case is indicated by the red line.

III. RESULTS

Under inversion conditions, a potential well is formed and the carrier density maximum shifts from the middle of the channel towards the surface. This electrostatic confinement towards the NW surface causes strong variations in the dispersion relations. The variations are different for different NW transport orientations. Figures 3a, 3b, and 3c show the dispersion of the [110] NW under low bias conditions, inversion, and strong inversion, respectively. As holes are confined on the surface, and the Fermi level (red line) is pushed into the subbands, the dispersion acquires lighter subbands at the high energies around the Fermi level relevant for transport. The same is observed for the [111] NW in Fig. 4. Previous works have shown that the subbands of the [110] and [111] NWs become lighter under structural cross section confinement. This reduces their effective mass and provides an advantage in their transport capabilities [8, 9, 13]. The interesting point, however, is that in these two cases the bands become lighter under electrostatic confinement as well. This behavior, on the other hand, is not observed for the [100] NW. Other than a change in the density of the subbands, the [100]

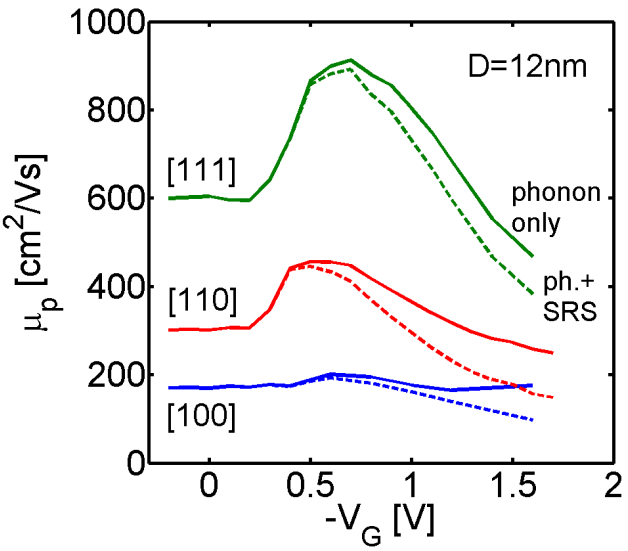

Figure 6: Low-field hole mobility for NWs of D=12nm in the [100], [110], and [111] transport orientations versus gate bias (-V_G). Solid lines: Phonon-limited mobility. Dashed lines: Phonon plus surface roughness scattering-limited mobility.

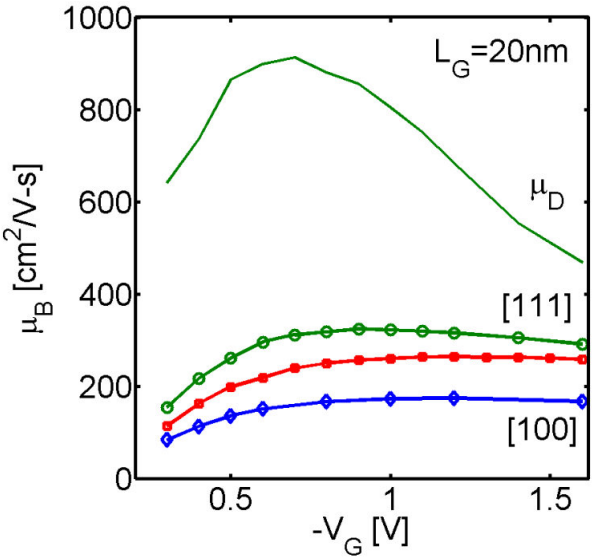

Figure 7: Solid lines: Hole "ballistic" mobility for NWs of D=12nm in the [100] (blue), [110] (red), and [111] (green) transport orientations versus gate bias (-V_G). Channel length L_G=20nm is assumed. Dashed line: The diffusive mobility of the [111] NW case, same as in Fig. 6.

NW does not undergo significant curvature variations with electrostatic gating as shown in Fig. 5.

The change in the bandstructure under electrostatic confinement has consequences in the NWs' mobility as shown in Fig. 6. The formation of the lighter subbands causes the mobility to increase by almost ~50% with increasing -V_G in the cases of the [111] and [110] NWs (solid lines). Such behavior is in contrast to the usual trend, which dictates that the mobility drops monotonically with -V_G. A mobility peak is reached around V_G=-0.7V. At stronger inversion, however, the mobility decreases because more and heavier subbands start to participate in transport near the Fermi level (see red lines (E_F) in Fig. 3c, Fig. 4c, and Fig. 5c). This increases scattering and causes mobility reduction, as also reported for thin p-type layers [16]. We also note that a strong mobility anisotropy is observed in the entire V_G range, with the [111] NW having ~2x and ~3x higher mobility compared to the [110] and [100] NWs, respectively.

For short channel semi-ballistic transistors, however, the diffusive mobility definition loses its validity. The measured mobility in a classical (and short channel) MOSFET is better explained by the combination of the diffusive and the so called "ballistic" mobility defined as $\mu_B = L_G / C_{OX}(V_G - V_T)R_{CH}$ [17]. In this expression L_G is the channel length, C_{OX} is the oxide capacitance, and V_T is the threshold voltage. The "ballistic" mobility depends on the channel resistance R_{CH}, extracted from the slope of the I_D-V_D curve at high V_G. In Ref. [17] we have indicated that even under zero series resistance, in low dimensional channels the "ballistic" mobility is limited to a few hundred cm^2/Vs. This is a consequence of the quantum resistance h/q_0^2 associated with each quantum mechanical mode that the carriers occupy. Here, h is Planck's constant. For 3D channels, this quantity is not important since when a lot of modes contribute to transport its value is minimized. For 1D (and 2D) channels, however, the value of the quantum resistance can be large enough to affect transport. The slope of the I_D-V_D for low V_D and high V_G is determined by the series combination of the quantum resistance and the channel resistance. As the channel is shortened, the channel resistance is reduced (and completely eliminated in the ballistic case), and the only resistance that remains is the quantum resistance. Because of this low dimensional effect, when extracting the mobility for 1D channel transistors using the usual method from the slope of the linear region of the I_D-V_D, one will extract a smaller value compared to the one expected from the intrinsic part of the channel alone. The computed ballistic mobility μ_B versus -V_G for the NWs in the three orientations is shown in Fig. 7. Its magnitude is lower than the diffusive mobility in Fig. 6 (also shown by the solid line in Fig. 7 for the [111] NW case), and its trend is different.

The "ballistic" mobility will be more relevant for short channels, whereas the diffusive mobility is important for long channels. This is demonstrated in Fig. 8, which shows the total mobility μ_{TOT} (so called "apparent" mobility) at inversion conditions (V_G=-0.6V) versus channel length L_G. This quantity is calculated from the diffusive and ballistic mobilities using Matthiesen's rule as $1/\mu_{TOT} = 1/\mu_D + 1/\mu_B$ [18, 19, 20, 21]. For longer channels, the mobility approaches the diffusive mobility values (peaks of Fig. 6), whereas it approaches the "ballistic" mobility values as the channels shortens (Fig. 7 values). For short channels, the actual mobility is significantly smaller that the intrinsic mobility (dotted line in Fig. 7 for the [111] NW), and some part of the benefit from anisotropy of the mobility in [111] and [110] NWs is lost. Nevertheless, even in the case of scaled channels, mechanisms that provide diffusive mobility improvements can improve the ballisticity of the

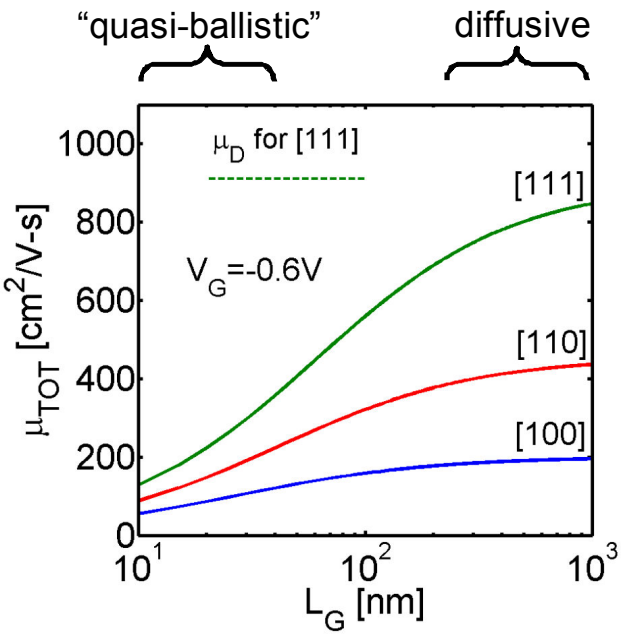

Figure 8: Total hole "apparent" mobility for NWs of D=12nm in the [100] (blue), [110] (red), and [111] (green) transport orientations versus channel length L_G at V_G=-0.6V.

device by achieving quasi-ballistic behavior at longer channel lengths, and improve the speed of transistors.

IV. Conclusions

The $sp^3d^5s^*$ atomistic tight-binding model is self-consistently coupled to the Poisson equation and linearized Boltzmann transport for the calculation of mobility in p-type silicon NWs. We show that the phonon-limited low-field mobility in p-type [110] and [111] NWs has a strong gate bias dependence and can increase by ~50% as the channel is driven into inversion. This increase is accounted on bandstructure changes upon electrostatic confinement. The mobility results are relevant for diffusive devices, whereas for short close to ballistic channels, the total mobility ("apparent" mobility) is influenced by the "ballistic" mobility, and which lower than its diffusive component, and it is itself lower. The large orientation variations are then also partially smeared out. Nevertheless, larger diffusive mobility corresponds to large mean free paths for scattering and larger channel ballisticity, which improves performance.

Acknowledgment

The work leading to these results has received funding from the European Community's Seventh Framework Programme under grant agreement no. FP7-263306 and the Austrian Science Fund, project P25368.

References

[1] ITRS Public Home Page. http://www.itrs.net/reports.html

[2] N. Singh et. al., "Ultra-narrow silicon nanowire gate-all-around CMOS devices: Impact of diameter, channel-orientation and low temperature on device performance," *In. Elec. Dev. Meeting*, 2006.

[3] K. H. Cho, *et* al., "Experimental evidence of ballistic transport in cylindrical gate-all-around twin silicon nanowire metal-oxide-semiconductor field-effect transistors," *Appl. Phys. Lett*., 92, 052102, 2008.

[4] M. Kobayashi and T. Hiramoto, "Experimental study on quantum confinement effects in silicon nanowire metal-oxide-semiconductor field-effect transistors and single-electron transistors," *J. Appl. Phys.*, 103, 053709, 2008.

[5] Bangsaruntip *et* al., *VLSI Symposium*, 2010.

[6] Y. Cui, Z. Zhong, D. Wang, W. U. Wang, and C. M. Lieber, "High performance silicon nanowire field effect transistors," *Nano Lett.*, 3, 149, 2003.

[7] K. Trivedi, H. Yuk, H. C. Floresca, M. J. Kim, and W. Hu, "Quantum confinement induced performance enhancement in sub-5-nm lithographic Si nanowire transistors," *Nano Lett.*, 11, 1412, 2011.

[8] A. K. Buin, A. Verma, A. Svizhenko, and M. P. Anantram, "Significant Enhancement of Hole Mobility in [110] Silicon Nanowires Compared to Electrons and Bulk Silicon," *Nano Lett.*, vol. 8, no. 2, pp. 760-765 (2008).

[9] N. Neophytou and H. Kosina, "Large enhancement in hole velocity and mobility in p-type [110] and [111] silicon nanowires by cross section scaling: An atomistic analysis," *Nano Lett.*, vol. 10, no. 12, pp. 4913-4919, 2010.

[10] N. Neophytou, A. Paul, M. Lundstrom, and G. Klimeck, "Bandstructure effects in silicon nanowire electron transport," *IEEE Trans. Elect. Dev.*, vol. 55, no. 6, pp. 1286-1297, 2008.

[11] T. B. Boykin, G. Klimeck, and F. Oyafuso, "Valence band effective-mass expressions in the sp3d5s* empirical tight-binding model applied to a Si and Ge parametrization," *Phys. Rev. B*, 69, 115201, 2004.

[12] A. Rahman, J. Guo, S. Datta, and M. Lundstrom, "Theory of ballistic nanotransistors," *IEEE Trans. Electron Devices*, 50, 1853, 2003.

[13] N. Neophytou, S. G. Kim, G. Klimeck, and H. Kosina, "On the Bandstructure Velocity and Ballistic Current of Ultra Narrow Silicon Nanowire Transistors as a Function of Cross Section Size, Orientation and Bias," *J. Appl. Phys.*, 107, 113701, 2010.

[14] N. Neophytou and H. Kosina, "Atomistic simulations of low-field mobility in Si nanowires: Influence of confinement and orientation," *Phys. Rev. B*, 84, 085313, 2011.

[15] N. Neophytou, O. Baumgartner, Z. Stanojevic, and H. Kosina, "Bandstructure and Mobility Variations in p-type Silicon Nanowires under Electrostatic Gate Field," *Solid State Electronics*, 2013.

[16] L. Donetti, F. Gámiz, S. Thomas, T. E. Whall, D. R. Leadley, P.-E. Hellström, G. Malm, and M. Östling, "Hole effective mass in silicon inversion layers with different substrate orientations and channel directions," *J. Appl. Phys.*, 110, 063711, 2011.

[17] N. Neophytou, T. Rakshit, and M. Lundstrom, "Performance Analysis of 60nm gate length III-V InGaAs HEMTs: Simulations vs. experiments," *IEEE Trans. Elect. Dev.*, 56, 1377, 2009.

[18] M. Luisier and G. Klimeck, "Phonon-limited mobility and injection velocity in n- and p-doped ultrascaled nanowire field-effect transistors with different crystal orientations," *In Proc. of Int. Elec. Dev. Meeting*, IEDM, 861, 2010.

[19] E. Gnani, A. Gnudi, S. Reggiani, and G. Baccarani, "Effective Mobility in Nanowire FETs Under Quasi-Ballistic Conditions," *IEEE Trans. Electr. Dev.*, 57, 336, 2011.

[20] R. Wang, H. Liu, R. Huang, J. Zhuge, L. Zhang, D.-W. Kim, X. Zhang, D. Park, and Y. Wang," Experimental Investigations on Carrier Transport in Si Nanowire Transistors: Ballistic Efficiency and Apparent Mobility," *IEEE Trans. Electr. Dev.*, 55, 2960, 2008.

[21] C. Jeong, D. A. Antoniadis, and M. S. Lundstrom, "On Backscattering and Mobility in Nanoscale Silicon MOSFETs," *IEEE Trans. Electr. Dev.*, 56, 2762, 2009.